RESEARCH PAPER

Ag-Au alloy nanoparticles prepared by electro-exploding wire technique

Abdullah Alqudami · S. Annapoorni · Govind · S. M. Shivaprasad

Received: 1 August 2007/Accepted: 17 November 2007/Published online: 6 December 2007 © Springer Science+Business Media B.V. 2007

Abstract Homogenous Ag-Au alloy nanoparticles having an average size of 12 ± 2 nm were successfully prepared by the exploding wire technique comprising of a wire-plate system and using 12 V batteries. The X-ray photoelectron spectroscopy data reveal the formation of alloy nanoparticles with Ag80-Au20 composition, which agrees with the absorption data, obtained using UV-Visible spectroscopy. XPS also reveals a thin metal-oxide shell on the metallic alloy core. These alloy nanoparticles show visible fluorescence emission that was compared with the observed fluorescence from pure Ag nanoparticles. A mechanism for the observed fluorescence is also provided.

Keywords Ag–Au alloy nanoparticles · Electro-exploding wire · XPS · SPR · Fluorescence · Synthesis · Nanocomposites

A. Alqudami (⋈) · S. Annapoorni Department of Physics and Astrophysics, University of Delhi, Delhi 110 007, India e-mail: aalqudami@physics.du.ac.in

Govind · S. M. Shivaprasad Surface Physics & Nanostructures Group, National Physical Laboratory, Dr. K S Krishnan Road, New Delhi 110 012, India

Introduction

Metal alloy nanoparticles are of great interest in surface science since they can exhibit electronic, optical and catalytic properties that are quite different from those of their constituents (Toshima and Yonezawa 1998; Rao 1998; Wang et al. 2005a,b Hannemann et al. 2006).

An important phenomenon that occurs on alloy surfaces is the segregation by which the surface chemical composition is completely modified. Some of the factors affecting the surface segregation of an alloy AB (Rao 1998) are; (1) Bond strengths (A–A, A–B and B–B), (2) Atomic size of the individual components A and B, (3) Enthalpies of sublimation and (4) Surface energies. In the case of nanostructured alloy particles, there are some additional factors that influence the final surface composition. They are preparation conditions, miscibility of the individual components at the atomic level and kinetics of reduction of the individual components.

The structure of Ag–Au alloy nanoparticles has generated a lot of interest since it is known that both Au and Ag have very similar lattice constants and are completely miscible over the entire composition range, forming homogeneous alloys in the bulk phase (Link et al. 1999). The choice of Ag and Au for many studies on metal nanoparticles is due to their full miscibility and high chemical stability, so that they can be used in almost any environment with no risk of rapid chemical reactions.



Moreover, the optical absorption spectra of Ag-Au alloy nanoparticles generally exhibit one surface plasmon resonance (SPR) band whose maximum depends on the alloy composition. Although the values of the free electron plasmon frequency (ω_p) are almost equal, the difference in the positions of the surface plasmon for Ag and Au is mainly due to the differing contributions of the interband transitions to the dielectric functions of the two metals (Moskovits et al. 2002). The surface plasmon oscillation in alloy particles is a hybrid resonance resulting from excitations of conduction as well as the d-band electrons (Link et al. 1999). It was also found that a synergistic effect exists between Au and Ag, leading to higher activity and hence a catalytic behavior. Gold is very useful as an alloying metal due to its relatively low reactivity. It has been used in conjunction with metals such as palladium, platinum and silver. Indeed, biomolecules have strong affinities to bind to both gold and silver nanoparticle surfaces. This would allow the use of Ag-Au alloy nanoparticles in a variety of biomedical applications.

Ag-Au alloy nanoparticle preparation has been achieved using various physical and chemical methods. For example, Papavassiliou (1976) obtained Ag-Au alloy colloid nanoparticles (~10 nm) of different composition using the arc-discharge method in 2butanol using two Pt electrodes, one of them was covered by melted Ag-Au alloy. These alloy colloids were used to study their SPR behavior. Lee et al. (2001) have produced Ag-Au alloy nanoparticles of 10 nm sizes by using pulsed laser irradiation of bulk alloy metals in water. Similarly, Ag₅₃ Au₄₇ of sizes about 22 nm have been prepared by laser vaporization controlled condensation (Abdelsayed et al. 2006). Chemically, Ag-Au alloy nanoparticles have also been prepared by co-reduction of HAuCl₄ and AgNO₃ using various reducing and capping agents (Link et al. 1999; He et al. 2002; Mallin and Murphy 2002; Raveendran et al. 2006) and in water-in-oil microemulsions of water/Aerosol OT/isooctane (Chen and Chen 2002). Various composition of these alloy colloids with size range between 8 and 35 nm were also synthesized by the addition of silver ions to a polymer protected aqueous gold sol in presence of a seeding agent followed by a heat treatment (Suyal et al. 2003). The alloy composition was also achieved using a biochemical method in a foam matrix using bovine serum albumin (BSA) protein (Singh et al. 2005).

The electro-exploding wire (EEW) technique has been extensively used to prepare pure metal nanoparticles (Sen et al. 2003b; Alqudami Annapoorni 2005, 2007; Alqudami et al. 2007). The plasma state was reached during the melting-evaporation process of the wire. This in fact made us feel that the explosion of two wires in one process would result in the formation of their alloy particles. This research article is an attempt to: (1) Make silver-gold alloy nanoparticles using the EEW technique, (2) Use the X-ray photoelectron spectroscopy (XPS) and the surface plasmon resonance techniques to analyze the resulting composition, (3) Study the structural properties of the particles using XRD and TEM and (4) Investigate their fluorescence behavior.

Experiment

Silver and gold wires (99.998%; Alfa Aesar) of 0.2 mm diameter and of length 20 mm were put jointly into the explosion circuit shown in Fig. 1 as a

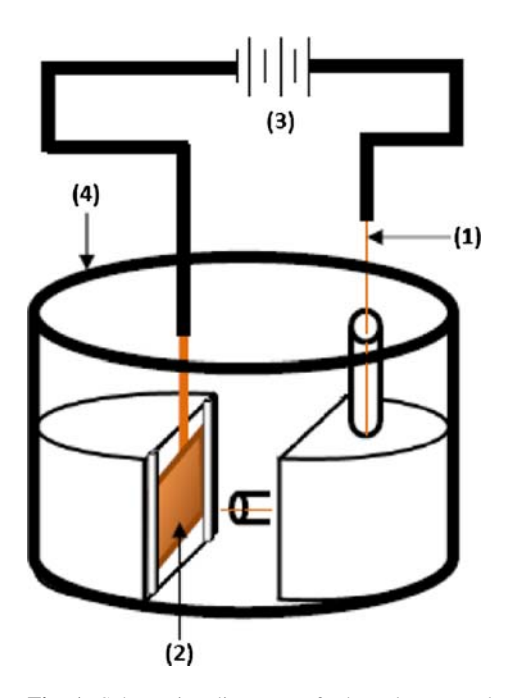


Fig. 1 Schematic diagram of the electro-exploding wire (EEW) set up (1) Thin metal wire, (2) Metal plate, (3) 36 V batteries and (4) Glass vessel



first electrode. The first electrode is connected to 36 V DC (12 volts batteries connected in series) and from the batteries to a silver plate (20, 20, 2) mm (99.998%; Alfa Aesar) as the second electrode. The wires to be exploded were driven through a wire guide made of glass. The silver plate was held with a hard plastic holder. Both the wire guide and the plate holder were fixed in a glass vessel filled with 100 ml of double distilled water. The electrical circuit remains open until the contact is made by the wire onto the plate manually, resulting in the wire explosion through a non-linear process (Vandana and Sen 2005), in a very short time. This in turn opens up the circuit for another explosion process. Details of the set up are published elsewhere (Sen et al. 2003a, 2003b, 2004, 2007). The alloy nanoparticles which disperse in the water solution were used as prepared for further analysis.

Results and discussion

A few drops from the nanoparticle suspension were dried on glass substrate for recording X-ray diffraction (XRD) data in the range 30–90°. The XRD was performed with a PW3710 Philips Analytical X-Ray Diffractometer using a Cu- K α radiation ($\lambda=1.54056$ Å). Figure 2 shows the obtained XRD patterns for the prepared nanoparticles. Peaks were observed at two theta degrees of 38.19°, 44.37°, 64.55°, 77.41° and 81.75° and have been indexed to (hkl) values of (111), (200), (220), (311) and (222), respectively.

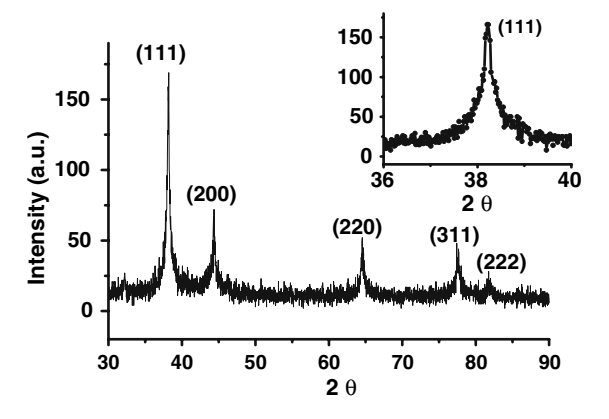


Fig. 2 X-ray diffractions of Ag-Au alloy nanoparticles (inset shows diffraction from the (111) plane)

The hkl values are corresponding to the FCC structure with the lattice constant of 4.08 \pm 0.005 Å. The Ag and Au have very similar lattice parameters. The lattice constants are 4.0862 Å (Ag) and 4.07825 Å (Au), and the nearest-neighbor interatomic distances are 2.889 (Ag-Ag) and 2.884 Å (Au-Au) for coordination number 12 (Bayler et al. 1996). The diffractogram of the Ag–Au combinations shows broad bands and this might probably be due to both the alloy formation and the small particle size. In order to look for a probable doublet, the 100% peak corresponding to (hkl) (111) was scanned between 36 and 41 degrees. There was no splitting observed as seen from the inset in Fig. 2, suggesting that the explosions have not yielded Ag and Au nanoparticles separately but probably an alloying might have occurred.

The particle size as estimated using Debye Scherrer's formula is found to be about 15 ± 1 nm.

In order to characterize the nanoparticles using Transmission Electron Microscope (TEM), a part from the water solution containing Ag–Au nanoparticles was sonicated for 15 min. A single micro-drop from the sonicated solution was allowed to dry on a carbon-coated copper grid for electron microscopy imaging using JEOL JEM 2000EX Transmission Electron Microscope. Figures 3a, b shows the TEM images of the Ag–Au alloy nanoparticles taken at low and high magnifications, respectively.

The alloy nanoparticles are spherical in shape. The size distributions of the particles that appear in the images (a, b) are shown in Figs. 3c, d, respectively. These size histogram have been obtained using Image-J 1.32j (USA) software. The size histograms show a lognormal size distribution with peak at about 12 ± 2 nm. This is in agreement with the size estimated from the XRD (15 \pm 1 nm).

The X-ray diffraction studies and the TEM measurements are techniques which are used only to determine the structure and size of the particles. Thus another technique should be used to investigate the composition of the prepared nanoparticles.

In order to investigate the possibility of alloy formation of Ag-Aunanoparticles, the X-ray photoelectron spectroscopy was performed. For the XPS measurements a part of the colloid was centrifuged at 10,000 rpm, re-dispersed in ethanol and allowed to dry on a cleaned silicon substrate. The analysis was done by the XPS system of Perkin–Elmer model 1257



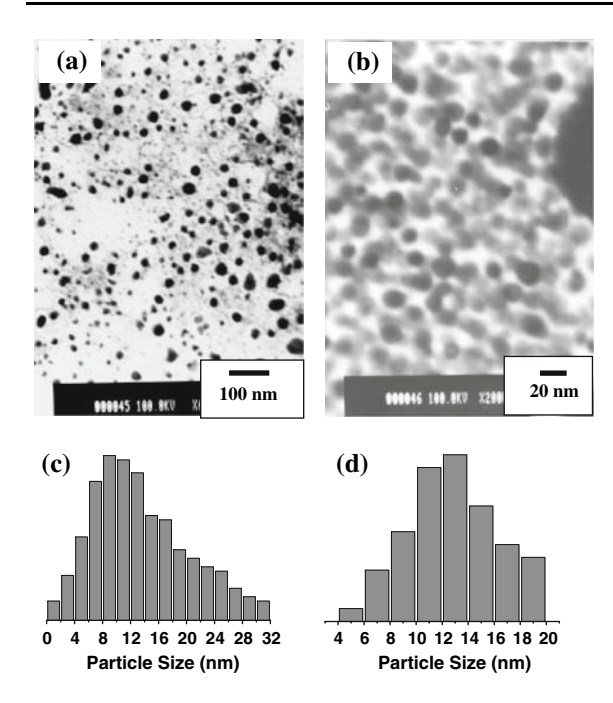


Fig. 3 (**a**, **b**) Transmission electron micrographs of the Ag–Au alloy nanoparticles at low and high magnification respectively, (**c**, **d**) Particle size distributions estimated for particles appear in the corresponding image

(Chakraborty et al. 2000), which consists of a dual anode X-ray source for primary beam (Mg K α /Al K α), a high resolution Hemispherical Electron Energy Analyzer and a 0–5 keV Ar+ ion source for sputtering. The sample under analysis was mounted on a high precision x, y, z, θ manipulator inside a UHV chamber of base pressure 5 × 10⁻¹⁰ Torr. The XPS analysis was done using the Al K α source, and the secondary electrons emitted were analyzed with the analyzer normal to the sample surface.

The surface of the sample under investigation was sputter cleaned by using Ar+ ion source of 4 kV, 20 mA emission current, for 2 min at an etching rate of approximately 1 nm per minute. As one is not aware of the components available in the sample a survey scan is performed for a large energy range. Figure 4 shows the XPS survey scan in the range 0–600 eV. Peaks of Ag and Au along with peaks of Carbon and Oxygen are observed. Binding energies (BE) corresponding to Au $(4f_7)$, Au $(4d_5)$, Ag $(3d_5)$, and Ag $(3p_3)$ were observed. Contamination peaks of C 1s and O 1s were observed at 285.6 and 531.6 eV respectively. To compensate for the charging effect, the binding energies were corrected to the standard

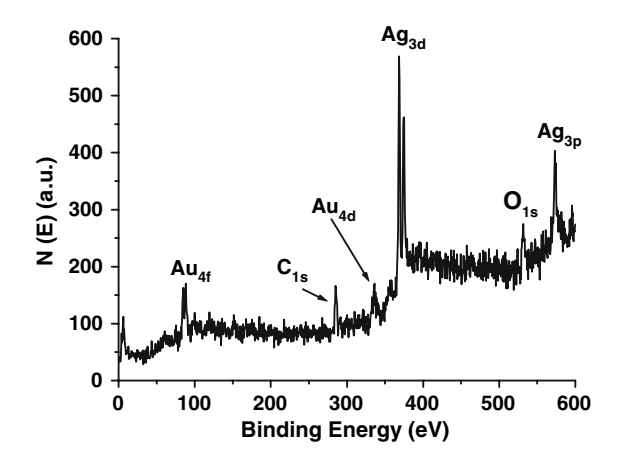


Fig. 4 XPS survey spectra obtained for the Ag-Au alloy nanoparticles after etching for 3 min

position of C 1s which was used as an internal standard (Wagner et al. 1979). Figure 5 shows the high resolution core-level spectra of Ag 3d and Au 4f obtained from the as prepared and etched samples, along with standard spectra of pure Ag and Au (Wagner et al. 1979), for comparison.

The summary of the analysis of the XPS date are listed in Table 1. After Ar ion etching, the BE's of Ag $3d_{5/2}$ and Au $4f_{7/2}$ were observed to be higher by about 0.2 and 0.3 eV respectively. The shift in BE to higher values could be due to the removal of some oxides from the surface of the nanoparticles (Murray 2005).

The XPS analyses allows one to estimate the composition ratio of the constituent materials namely Ag and Au using the integrated areas I_{Ag} and I_{Au} of the BE peaks $3d_{5/2}$ and $4f_{7/2}$ respectively and the atomic sensitivity factor (ASF) (Wagner et al. 1979) as,

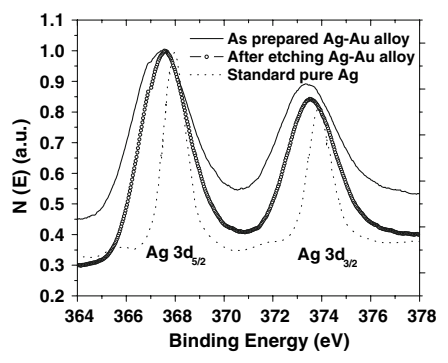
$$\frac{C_{Ag}}{C_{Au}} = \frac{I_{Ag}/ASF_{Ag}}{I_{Au}/ASF_{Au}}$$

The composition ratios of the Ag and Au in the alloy nanoparticles were estimated to be (78.6:21.4) % and (80:20) % (\pm 1%) corresponding to (Ag:Au) composition before and after etching respectively.

The BE values obtained from the XPS analysis of the Ag-Au alloy nanoparticles are in good agreement with literature (Wang et al. 2005a, b; Kariuki et al. 2006; Kim 2003; Sandhyarani and Pradeep 2000). The shift in the BE of the Ag-Au alloys from those of pure forms, (Barrie and Christensen, 1976; Fuggle



Fig. 5 High resolutions XPS Ag 3d and Au 4f spectra obtained from Ag— Au alloy nanoparticles compared with the standard spectra of pure Ag and Au



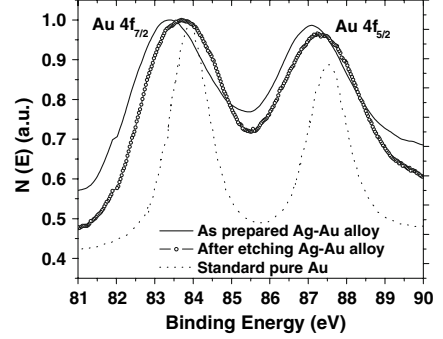


Table 1 Binding energies (BE) and FWHM in eV for Ag-Au alloy nanoparticles compared with pure form of Ag and Au

	B. E. (eV)		FWHM (eV)	
	$3d_{5/2}$	3d _{3/2}	$3d_{5/2}$	3d _{3/2}
Ag ^a	367.9	373.9	1.14	1.23
$(1)^{b}$	367.4	373.4	2.63	2.91
(2) ^c	367.6	373.6	2.33	2.46
	B. E. (eV)		FWHM (eV)	
	4f _{7/2}	4f _{5/2}	4f _{7/2}	4f _{5/2}
Au ^a	83.8	87.45	1.31	1.42
$(1)^{b}$	83.4	87.15	2.28	2.38
(2) ^c	83.7	87.35	2.38	2.60

^a Pure standard form

and Martensson, 1980), is an indication of the alloy nanoparticles formation (Tyson et al. 1992; Kim 2003). As discussed by Hoflund et al. (2000), the relatively high FWHM of the XPS peaks is attributed to the presence of some oxidation states.

The binding energy of C 1s in the present investigation was observed at about 285.6 eV. The carbon peak is attributed to contamination from the pumps.

Oxygen is likely to be in the form of thin oxide layer formed during the growth of the alloy nanoparticles and their interactions with the water molecules.

The optical absorption studies have been performed on the Ag–Au alloy nanoparticles and compared with the optical response of pure Ag nanoparticles which have been prepared by the same technique and are reported elsewhere (Alqudami and

Annapoorni 2007). Both the nanoparticle systems were studied in the water solution form with appropriate base-line corrections and using quartz cells. Both the solutions were sonicated for 10 minutes prior to the optical studies. The absorptions have been recorded in the wavelength range of 200–700 nm using a Shimadzu UV-2510PC spectrophotometer and the spectra are shown in Fig. 6. It has been observed that the Ag–Au nanoparticles have only one surface plasmon absorption band centered at about 424 nm and that reported for Au is about 520 nm. The SPR band of pure Ag is observed to be at about 404 nm. The SPR peak of the Ag–Au nanoparticles is red-shifted by about 20 nm compared with pure Ag nanoparticles.

In fact, the optical absorption of the nanoparticles showed a clear evidence of the Ag–Au alloy nanoparticles formation. It is well known that Ag and Au nanoparticles have plasmon absorption bands at about 400 and 520 nm respectively. The physical mixture

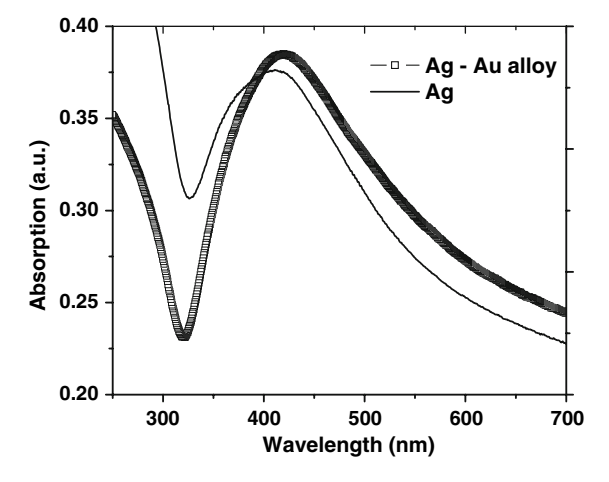


Fig. 6 Surface plasmon resonance (SPR) of Ag-Au alloy nanoparticles compared with Ag nanoparticles



b As prepared Ag-Au alloy nanoparticles

^c Ag-Au alloy nanoparticles, after etching

of Ag and Au monometallic nanoparticles are expected to have two plasmon bands. The formation of Ag–Au alloy nanoparticles could be deduced from the fact that the optical absorption shows only one SPR band. This band is highly influenced by the composition percentage (Lee and El-Sayed 2006; Papavassiliou 1976; Hostetler 1998; Chen and Chen 2002; Lee et al. 2001; Kim et al. 2003; Raveendran et al. 2006; Wang et al. 2005a, b; Link et al. 1999; Abdelsayed et al. 2006; Hubenthal et al. 2005; Suyal et al. 2003; Singh et al. 2005; Shibata et al. 2002; He et al. 2002; Philip et al. 2000; Sloufova et al. 2004; Agrawal et al. 2006; Mallin and Murphy 2002).

The SPR peaks were observed at 404 and 424 nm for Ag nanoparticles and Ag-Au alloy nanoparticles respectively. The composition percentage can be calculated using the absorption peak shift. It was reported that plasmon maximum was red shifted almost linearly from 400 to 520 nm with increasing Au content (Papavassiliou 1976; Mallin and Murphy 2002; Chen and Chen 2002; Lee et al. 2001; Raveendran et al. 2006; Wang et al. 2005a, b; Link et al. 1999).

The percentage composition of Ag-Au alloy was also estimated using the optical/SPR absorption. This was done by simulating the extinction cross section using Mie's theory and the details are described below.

The extinction cross sections of Ag-Au alloy nanoparticles in water medium (Refractive index: 1.334) have been calculated using the equation,

$$\sigma_{ext} = \frac{9 \cdot \mathbf{V} \cdot \varepsilon_{\mathrm{m}}^{3/2}(\omega)}{\mathbf{c}} \cdot \frac{\omega \cdot \varepsilon_{r}'(\omega)}{\left[\varepsilon_{r}'(\omega) + 2 \cdot \varepsilon_{m}(\omega)\right]^{2} + \varepsilon_{r}''(\omega)^{2}}$$

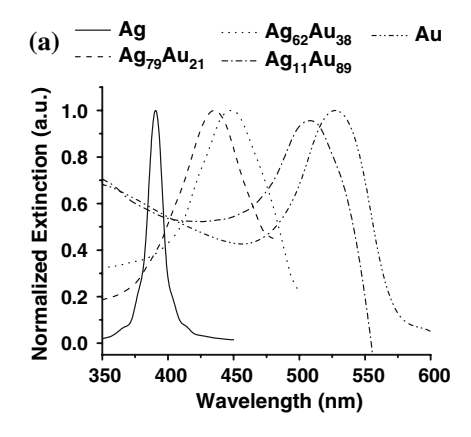
The simulation was performed for the alloy compositions of Ag₁₀₀ Au₀, Ag₇₉ Au₂₁, Ag₆₂ Au₃₈, Ag₁₁ Au₈₉ and Ag₀ Au₁₀₀. These compositions were chosen due to the availability of the dielectric functions data. Ripken (1972) determined the experimental optical constants (real and imaginary part of the dielectric function) on thin films (30-40 nm thickness) of silver, gold and their alloys. Using these reported data for the above mentioned alloy compositions, the extinction cross section spectra were generated and are shown in Fig. 7a. It is clearly observed that the SPR peak is shifting from that of silver (~ 395 nm) to that of gold (~ 525 nm) with increasing Au mole fraction. This shift is plotted against the Au mole fraction as shown in Fig. 7b. The data points were fitted linearly with resulting linear equation as:

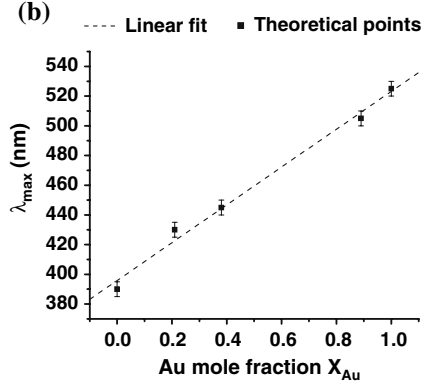
$$\lambda_{max}(nm) = 396(\pm 2) + 128(\pm 4)X_{Au}$$

Using the above equation and by substituting $\lambda_{max} = 424$ nm (as observed experimentally in Fig. 6), the X_{Au} value comes to be about 0.21 ± 0.02 . This value is in quite an agreement with the composition obtained using the XPS data $(X_{Au} = 0.2 \pm 0.01)$.

Ag nanoparticles obtained by EEW technique exhibited fluorescence emission at about 485 nm under plasmonic excitation (Alqudami and Annapoorni 2005; 2007). In this article, the water solution containing Ag–Au alloy nanoparticles has also been studied for its fluorescence behavior. The fluorescence behavior of the Ag–Au alloy nanoparticles is also compared with the fluorescence behavior of pure Ag nanoparticles. The excitation wavelengths for both

Fig. 7 (a) Mie extinction cross section spectra of the Ag–Au alloy nanoparticles at different compositions calculated using the dielectric functions of alloy thin films from Ripken (1972). (b) Plot of λ_{max} vs. Au mole fraction obtained from (a)







the systems (Ag–Au and Ag) have been decided based on the SPR absorption peaks. The Ag–Au alloy nanoparticles were excited at 424 nm and the Ag nanoparticles have been excited at 390 nm. The observed fluorescence excitation and emission spectra are shown in Fig. 8. Table 2 summarizes the observed emission bands of Ag and Ag–Au nanoparticles.

The emission is found to depend on the excitation wavelength. The main observations are: (1) Ag nanoparticles are to be excited at 390 nm while Ag–Au alloy nanoparticles at 424 nm, that is in agreement with the absorption spectra results discussed earlier. (2) No shift in the emission peak positions were observed in both the systems except the change in the relative intensity, indicating that the emission is dominated by the Ag contents. (3) The emissions at high energies (433, 450 nm) are associated with high energy excitation (390 nm).

The fluorescence from monometallic Ag and Au nanoparticles has been reported and reviewed (Ievlev et al. 2000; Zheng and Dickson 2002; Gangopadhyay

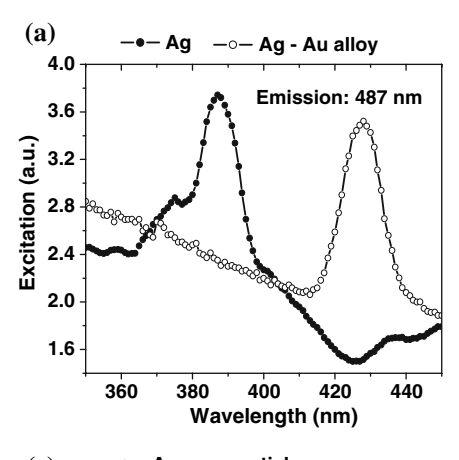
et al. 2005; Treguer et al. 2005; Jiang et al. 2005; Hwang et al. 2002; Geddes et al. 2003; Link and El-Sayed 2003). However, fluorescence from Ag–Au alloy nanoparticles, to the best of our knowledge, has not been reported earlier.

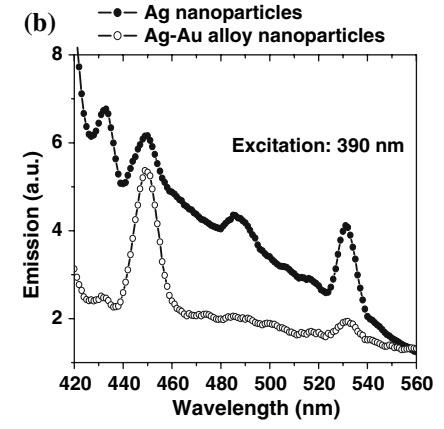
The origin of the fluorescence is the radiative transitions among the characteristic surface/interface energy bands. Nanoparticle suspensions have very large surface/interface active area, where chemisorption and/or physisorption process takes place. Localized surface electrons form discrete energy levels depending on the size, shape of the nanoparticles and the thickness of the adsorbed surface layer.

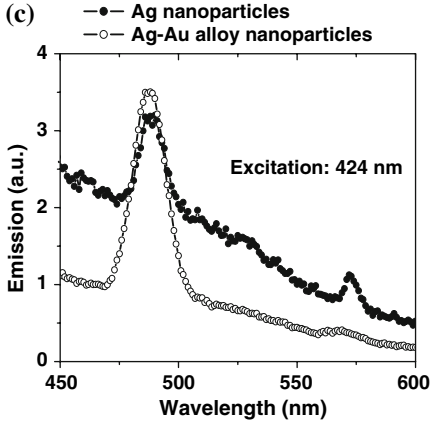
Table 2 Emissions of Ag and Ag-Au alloy nanoparticles at different excitations

	Emission (nm)	
	Ag	Ag ₈₀ – Au ₂₀
Excitation (nm)	433, 450, 486, 532 487, 572	431, 450, 532 487, 569

Fig. 8 Fluorescence of Ag–Au alloy nanoparticles compared with Ag nanoparticles; (a) Excitation spectra at emission wavelength of 487 nm (b and c) Emission spectra at excitation wavelengths of 390 nm, and 424 nm, respectively









Ag-Au alloy nanoparticles undergo selected raditransitions when compared nanoparticles. Au contents in the alloy nanoparticles perturb the d-band energy level and give rise to some favorable transitions. It was reviewed that d-band electrons of the noble metal nanoparticles absorb the incident photon energy and promote to higher electronic states in the sp-band. The electron-hole pair recombines un-radiatively through electronphonon scattering process but then may combine radiatively giving rise to the observed fluorescence (Link and El-Sayed 2003). Or the excited particle plasmons themselves can radiate and give rise to the observed emissions (Dulkeith et al. 2004).

The mechanism for alloying of small particles is still not clear. Kinetic considerations indicate that, for the two metals to mix, the diffusion coefficient needs to be many orders of magnitude larger than for the bulk materials (Yasuda and Mori 1992; Yasuda et al. 1993). The surface melting plays an important role (Shimizu et al. 2001), especially with relatively small nanoparticles (~ 100 atoms). A process driven by surface free energy also leads to migration of atoms at the nanoparticles surface (Schmid et al. 2000). Since the melting temperature of the smaller particles is much lower than the corresponding bulk, much faster inter-diffusion of the atoms is expected in the nanoparticles. A number of studies on mechanical alloying have suggested that interfacial imperfections enhance the diffusion by many orders of magnitude (Das et al 1999).

A study of the literature shows that wire explosion and fragmentation generally tend to proceed in the following manner (Vandana and Sen 2005): heating of wire and wire melting; wire explosion (evaporation) and formation of a high density core surrounded by low density ionized corona; coronal compression by self-induced magnetic fields; and fast expansion of explosion products.

We have evidence of plasma formation, as the electro-explosion process is accompanied by emission of visible light. The exploding wires-plate system brings both the wire and plate surface instantaneously to their melting points (typically after 140 μ s). This melting process brings both the wires (silver and gold) as well as the plate at the contact point to a mix or alloy state before they evaporate. The evaporated atoms, ions or clusters then continue to grow and form alloy nanoparticles.

Inter-diffusion will proceed to further form random alloy nanoparticles.

To explain the expected atomic diffusion, we invoke a relatively high density of defects, particularly vacancies, at the bimetallic interface. Such defects may be caused by the surface curvature or by the need to stabilize the particle during the synthesis process. The diffusion in metals is commonly accepted to proceed via migration of atoms into vacancy defects. A single vacancy at the interface is enough to catalyze the fast diffusion rate (Sheng and Ma 2001). Water medium in the present work may induce additional strain into the lattice and enhance migration of the atoms.

Conclusion

The exploding wire technique can be used not only to prepare pure metal nanoparticles, but can also be used to prepare metal alloy nanoparticles. In this research article we have shown the successful preparation of fluorescent Ag₈₀-Au₂₀ alloy nanoparticles. The XPS data analysis and the SPR behavior of the nanoparticles were used to confirm the formation of alloy structures. This technique can be tried for other metallic combinations and composition percentages which might allow further understanding of the mechanism for alloying of small particles. The composition percentage can be controlled through the selection of wires of different diameters and the plate material, which is at present being carried out.

Acknowledgements We would like to acknowledge the Department of Science and Technology (DST), India for the funding through the project (SR/S5/NM-52/2002) from the Nanoscience and Technology Initiative programme.

References

Abdelsayed V, Saoud KM, El-Shall MS (2006) Vapor phase synthesis and characterization of bimetallic alloy and supported nanoparticle catalysts. J Nanopart Res 8:519–531

Agrawal VV, Mahalakshmi P, Kulkarni GU, Rao CNR (2006) Nanocrystalline films of Au–Ag, Au–Cu, and Au–Ag–Cu alloys formed at the organic-aqueous interface. Langmuir 22:1846–1851

Alqudami A, Annapoorni S (2005) Fluorescent silver nanoparticles via exploding wire technique. Pramana J Phys 65:815–819



- Alqudami A, Annapoorni S, Lamba S, Kothari PC, Kotnala RK (2007) Magnetic properties of iron nanoparticles prepared by exploding wire technique. J Nanosci Nanotechnol 7:1898–1903
- Barrie A, Christensen NE (1976) High-resolution X-ray photoemission spectra of silver. Phys Rev B 14:2442–2447
- Bayler A, Schier A, Bowmaker GA, Schmidbaur H (1996) Gold is smaller than silver. Crystal structures of [Bis(trimesitylphosphine)gold(I)] and [Bis(trimesitylphosphine)silver(I)] Tetrafluoroborate. J Am Chem Soc 118:7006–7007
- Chakraborty BR, Mohan P, Shivaprasad SM, Sharma DR, Anandan C, Gupta AC, Raychaudhuri AK (2000) Surface analytical facility at NPL, New Delhi. Curr Sci 78:1523– 1527
- Chen DH, Chen JC (2002) Formation and characterization of Au–Ag bimetallic nanoparticles in water-in-oil microemulsions. J Mater Chem 12:1557–1562
- Das D, Chatterjee PP, Manna I, Pabi SK (1999) A mechanism of enhanced diffusion kinetics in mechanical alloying of Cu-18 at.% Al by planetary ball milling. Scr Mater 41:861–866
- Dulkeith E, Niedereichholz T, Klar TA, Feldmann J, von Plessen G, Gittins DI, Mayya KS, Caruso F (2004) Plasmon emission in photoexcited gold nanoparticles. Phys Rev B 70:205424-1-4
- Fuggle JC, Martensson N (1980) Core-level binding energies in metals. J Electron Spectrosc Relat Phenom 21:275–281
- Gangopadhyay P, Kesavamoorthy R, Bera S, Magudapathy P, Nair KGM, Panigrahi BK, Narasimhan SV (2005) Optical absorption and photoluminescence spectroscopy of the growth of silver nanoparticles. Phys Rev Lett 94: 047403–1
- Geddes CD, Parfenov A, Gryczynski I, Lakowicz JR (2003) Luminescent blinking of gold nanoparticles. Chem Phys Lett 380:269–272
- Hannemann S, Grunwaldt J-D, Krumeich F, Kappen P, Baiker A (2006) Electron microscopy and EXAFS studies on oxide-supported gold-silver nanoparticles prepared by flame spray pyrolysis. Appl Surf Sci 252:7862–7873
- He ST, Xie SS, Yao JN, Gao HJ, Pang SJ (2002) Self-assembled two-dimensional superlattice of Au–Ag alloy nanocrystals. Appl Phys Lett 81:150–152
- Hoflund GB, Hazos ZF, Salaita GN (2000) Surface characterization study of Ag, AgO, and Ag₂O using X-ray photoelectron spectroscopy and electron energy-loss spectroscopy. Phys Rev B 62:11126–11133
- Hostetler MJ, Zhong CJ, Yen BKH, Anderegg J, Gross SM, Evans ND, Porter M, Murray RW (1998) Stable, monolayer-protected metal alloy clusters. J Am Chem Soc 120:9396–9397
- Hubenthal F, Ziegler T, Hendrich C, Alschinger M, Trager F (2005) Tuning the surface plasmon resonance by preparation of gold-core/silver-shell and alloy nanoparticles. Eur Phys J D 34:165–168
- Hwang YN, Jeong DH, Shin HJ, Kim D (2002) Femtosecond emission studies on gold nanoparticles. J Phys Chem B 106:7581–7584
- Ievlev D, Rabin I, Schulze W, Ertl G (2000) Light emission in the agglomeration of silver clusters. Chem Phys Lett 328:142–146

- Jiang Z, Yuan W, Pan H (2005) Luminescence effect of silver nanoparticle in water phase. Spectrochim. Acta A 61:2488–2494
- Kariuki NN, Luo J, Hassan SA, Lim IIS, Wang L, Zhong CJ (2006) Assembly of bimetallic gold-silver nanoparticles via selective interparticle dicarboxylate-silver linkages. Chem Mater 18:123–132
- Kim MJ, Na HJ, Lee KC, Yoo EA, Lee M (2003) Preparation and characterization of Au–Ag and Au–Cu alloy nanoparticles in chloroform. J Mater Chem 13:1789–1792
- Lee KS, El-Sayed MS (2006) Gold and silver nanoparticles in sensing and imaging: sensitivity of plasmon response to size, shape, and metal composition. J Phys Chem B 110:19220–19225
- Lee I, Han SW, Kim K (2001) Production of Au–Ag alloy nanoparticles by laser ablation of bulk alloys. Chem Commun 1782–1783
- Link S, El-Sayed MA (2003) Optical properties and ultrafast dynamics of metallic nanocrystals. Annu Rev Phys Chem 54:331–366
- Link S, Wang ZL, El-Sayed MA (1999) Alloy formation of gold-silver nanoparticles and the dependence of the plasmon absorption on their composition. J Phys Chem B 103:3529–3533
- Mallin MP, Murphy CJ (2002) Solution-phase synthesis of sub-10 nm Au-Ag alloy nanoparticles. Nano Lett 2: 1235–1237
- Moskovits M, Sloufova IS, Vlckova B (2002) Bimetallic Ag— Au nanoparticles: Extracting meaningful optical constants from the surface-plasmon extinction spectrum. J Chem Phys 116:10435–10446
- Murray BJ, Newberg JT, Walter EC, Li Q, Hemminger JC, Penner RM (2005) Reversible resistance modulation in mesoscopic silver wires induced by exposure to amine vapor. Anal Chem 77:5205–5214
- Papavassiliou GC (1976) Surface plasmons in small Au-Ag alloy particles. J Phys F: Metal Phys. 6:L103–105
- Philip R, Kumar GR, Sandhyarani N, Pradeep T (2000) Picosecond optical nonlinearity in monolayer-protected gold, silver, and gold-silver alloy nanoclusters. Phys Rev B 62:13160–13166
- Rao GR (1998) Chemistry of bimetallic surfaces. Curr Sci 75:901–910
- Raveendran P, Fu J, Wallen SL (2006) A simple and "green" method for the synthesis of Au, Ag, and Au–Ag alloy nanoparticles. Green Chem 8:34–38
- Ripken K (1972) The optical constants of Au, Ag and their alloys in the energy region from 2.4 to 4.4 eV. Z Phys 250:228-234
- Sandhyarani N, Pradeep T (2000) Crystalline solids of alloy clusters. Chem Mater 12:1755–1761
- Schmid AK, Bartelt NC, Hwang RQ (2000) Alloying at surfaces by the migration of reactive two-dimensional islands. Science 290:1561–1564
- Sen P, Ghosh J, Kumar P, Alqudami Abdullah, Vandana (2003a) Process and apparatus for producing metal nanoparticles (Indian Patent 840/Del/03); (2004) (PCT International Appl. No PCT/IN2004/000067); (2004) (International Publication No. WO 2004/112997); (2007) (US Patent Appl. No 20070101823)



- Sen P, Ghosh J, Alqudami Abdullah, Kumar P, Vandana (2003b) Preparation of Cu, Ag, Fe and Al nanoparticles by the exploding wire technique. J Chem Sci 115:499–508
- Sheng HW, Ma E (2001) Intermixing of a system with positive heat of mixing at high strain rates. Phys Rev B 63:224205-1-6
- Shibata T, Bunker BA, Zhang Z, Meisel D, Vardeman CF, Gezelter JD (2002) Size-dependent spontaneous alloying of Au-Ag nanoparticles. J Am Chem Soc 124:11989– 11996
- Shimizu Y, Ikeda K, Sawada S (2001) Spontaneous alloying in binary metal microclusters: a molecular dynamic study. Phys Rev B 64:075412-1-13
- Shon YS, Dawson GB, Porter M, Murray RW (2002) Monolayer-protected bimetal cluster synthesis by core metal galvanic exchange reaction. Langmuir 18:3880–3885
- Singh AV, Bandgar BM, Kasture M, Prasad BLV, Sastry M (2005) Synthesis of gold, silver and their alloy nanoparticles using bovine serum albumin as foaming and stabilizing agent. J Mater Chem 15:5115–5121
- Sloufova IS, Vlckova B, Bastl Z, Hasslett TL (2004) Bimetallic (Ag)Au nanoparticles prepared by the seed growth method: two-dimensional assembling, characterization by energy dispersive X-ray analysis, X-ray photoelectron spectroscopy, and surface enhanced Raman spectroscopy, and proposed mechanism of growth. Langmuir 20:3407–3415
- Suyal G, Mennig M, Schmidt H (2003) Synthesis of nanocomposite thin films containing Ag-Au alloy colloids for wavelength tenability. J Mater Sci 38:1645-1651
- Toshima N, Yonezawa T (1998) Bimetallic nanoparticlesnovel materials for chemical and physical applications. New J Chem 22:1179–1201

- Treguer M, Rocco F, Lelong G, Nestour AL, Cardinal T, Maali A, Lounis B (2005) Fluorescent silver oligomeric clusters and colloidal particles. Solid State Sci 7:812–818
- Tyson CC, Bzowski A, Kristof P, Kuhn M, Sammynaiken R, Sham TK (1992) Charge redistribution in Au-Ag alloys from a local perspective. Phys Rev B 45:8924–8928
- Vandana, Sen P (2005) Nanometre scale surface modification in a needle–plate exploding system. J Phys Condens Matter 17:5327–5334
- Wagner CD, Riggs WM, Davis LE, Moulder JF (1979) In: Muilenberg GE (ed) Handbook of X-ray photoelectron spectroscopy, A reference book of standard data for use in X-ray photoelectron spectroscopy, Perkin-Elmer Corp., Minnesota, USA
- Wang AQ, Chang CM, Mou CY (2005a) Evolution of catalytic activity of Au-Ag bimetallic nanoparticles on mesoporous support for co oxidation. J Phys Chem B 109:18860– 18867
- Wang AQ, Liu JH, Lin SD, Lin TS, Mou CY (2005b) A novel efficient Au–Ag alloy catalyst system: preparation, activity, and characterization. J Catal 233:186–197
- Yasuda H, Mori H (1992) Spontaneous alloying of zinc atoms into gold clusters and formation of compound clusters. Phys Rev Lett 69:3747–3750
- Yasuda H, Mori H, Komatsu M, Takeda K (1993) Spontaneous alloying of copper atoms into gold clusters at reduced temperatures. J Appl Phys 73:1100–1103
- Zheng J, Dickson RM (12002) Individual water-soluble dendrimer-encapsulated silver nanodot fluorescence. J Am Chem Soc 124:13982–13983

